

# Cellulose aero-, cryo- and xerogels: towards understanding of morphology control

Nela Buchtová · Tatiana Budtova

Received: 1 March 2016 / Accepted: 9 May 2016 / Published online: 12 May 2016  
© Springer Science+Business Media Dordrecht 2016

**Abstract** Highly porous, lightweight versatile cellulose materials were prepared via dissolution–coagulation and subsequent various drying routes. Cellulose was dissolved in ionic liquid/DMSO mixture and coagulation was performed in ethanol. The as prepared wet precursors were used to make materials with three different drying methods: supercritical CO<sub>2</sub> drying, freeze-drying and vacuum drying. The influence of cellulose concentration and drying method on the density, porosity, specific surface area and morphology of cellulose materials is presented and discussed. We provide the understanding of morphology development as a function of processing conditions and give the “recipes” for porosity control.

**Keywords** Cellulose · Freeze-drying · Supercritical CO<sub>2</sub> drying · Morphology · Specific surface area · Porosity

## Introduction

Cellulose, the most abundant, renewable, biocompatible and biodegradable natural polymer on Earth, is a

very promising raw material for replacing fossil based polymers and preparing novel value-added advanced functional materials (Klemm et al. 2005; Isikgor and Becer 2015). Cellulose can be shaped into various objects such as beads (Sescousse et al. 2011a; Trygg et al. 2013), fibers of various diameters from ten microns (viscose, Tencel) to few hundreds or tens of nanometers (Pääkkö et al. 2008; Kobayashi et al. 2014) and films (cellophane). The morphology and properties of these objects can be very different, from homogeneous materials with density close to 1.5 g/cm<sup>3</sup> (viscose and Tencel fibres, cellophane) to porous foams and aerogels with density around 0.01–0.2 g/cm<sup>3</sup> and high specific surface area of several hundreds of m<sup>2</sup>/g (Gavillon and Budtova 2008; Hoepfner et al. 2008; Pääkkö et al. 2008; Aaltonen and Jauhiainen 2009; Liebner et al. 2009; Sehaqui et al. 2011; Kobayashi et al. 2014). The latter materials are very attractive for various applications, from bio-medical (controlled release, scaffolds, matrices for cell growth) (García-González et al. 2011) to engineering (thermal insulation) (Kobayashi et al. 2014) and electrochemical when pyrolyzed (Guilminot et al. 2008). Each application requires specific morphology, and thus it is essential to understand and control pore size distribution, specific surface area and material density.

Highly porous cellulose can be prepared from cellulose I such as bacterial or micro- or nanofibrillated cellulose (Pääkkö et al. 2008; Liebner et al. 2010; Sehaqui et al. 2011; Kobayashi et al. 2014; Zhang et al. 2014) or from cellulose II via cellulose dissolution–

---

N. Buchtová · T. Budtova (✉)  
MINES ParisTech, CEMEF - Centre de Mise en Forme  
des Matériaux, CNRS UMR 7635, PSL Research  
University, CS 10207 rue Claude Daunesse,  
06904 Sophia Antipolis, France  
e-mail: tatiana.budtova@mines-paristech.fr

coagulation route (Gavillon and Budtova 2008; Hoepfner et al. 2008; Aaltonen and Jauhiainen 2009; Liebner et al. 2009; Sescousse et al. 2011b; Ganesan et al. 2016). In all cases the final step, drying, is of great importance as it determines material's morphology. If cellulose was not modified, evaporative drying usually leads to pores' collapse due to high capillary stresses. They depend mainly on liquid/gas surface tension, liquid/solid contact angle and pore size. Freeze-drying (or lyophilisation) and drying in supercritical (sc) conditions are known to preserve the open porosity of cellulose "wet gels". Freeze-drying is sublimation of the solid, usually frozen water, from the pores of a wet precursor. In sc conditions, liquid/gas surface tension is zero because there is no longer liquid/gas meniscus. However, the morphology of the porous material obtained after lyophilisation or sc drying is very different. Freeze-drying leads to the formation of large pores and channels from several microns to tens of microns (Sehaqui et al. 2010; Lee and Deng 2011; Zhou et al. 2014) due to the growth of ice crystals. Supercritical drying better preserves fine network structure leading to the formation of mesopores and small macropores which is reflected by specific surface area of several hundreds of  $\text{m}^2/\text{g}$  (Gavillon and Budtova 2008; Hoepfner et al. 2008; Aaltonen and Jauhiainen 2009; Liebner et al. 2009; Sescousse et al. 2011b).

In most of publications only one method of drying is used to make porous cellulose materials. To deduce the exact influence of drying on the morphology and properties is thus not easy as they also depend on several other preparation conditions such as cellulose molecular weight and pre-treatment, cellulose concentration and solvent used to dissolve it, gelation of solution or not and way of coagulation. Hoepfner et al. (2008) used both sc and freeze-drying but only specific surface areas were compared. An interesting study was performed recently by Ganesan et al. (2016): they used emulsion templating technique to make cellulose II based porous scaffold materials. These scaffolds were prepared by mixing cellulose–calcium thiocyanate solution with surfactant-in-oil, in the ratio 1:1. A creamy emulsion was obtained, and cellulose was coagulated in isopropanol followed by washing in ethanol. The morphology obtained, with interconnected highly macroporous channels of diameter of 100–300 microns, was very different from non-emulsified coagulated cellulose. The influence of the drying methods (sc drying, freeze-drying and ambient drying)

on scaffolds' morphology and mechanical properties was demonstrated, however, no influence of cellulose concentration was studied.

The goal of the present work was to perform a comprehensive study of the influence of drying conditions on the morphology and properties of porous cellulose starting from the same precursor. Several reasons motivated our work. It may often be found in literature that a lightweight polysaccharide is named "aerogel" whatever is the way of drying. Thus we wanted to demonstrate that sc drying and freeze-drying result in porous cellulose with very different morphology, and, consequently, using correct terminology is important. Another motivation was to investigate if oriented channel-like large pores obtained with unidirectional freeze-drying of polysaccharide solutions or suspensions (nanofibrillated cellulose or cellulose or chitosan whiskers) (Flauder et al. 2014; Sehaqui et al. 2010; Lee and Deng 2011; Köhnke et al. 2014; Zhou et al. 2014) would be reproduced for the case when a wet precursor is coagulated cellulose. Finally, to the best of our knowledge, there is no systematic study and comparison of the influence of cellulose concentration on the morphology and properties of cellulose aerogels and cryogels.

To reach these goals, three families of samples were prepared from the same precursors: so-called xerogels with low-vacuum evaporative drying, so-called cryogels with freeze-drying and aerogels with sc  $\text{CO}_2$  drying. Cryogels were obtained in two ways: homogeneous and unidirectional freezing. We also varied cellulose concentration from 3 to 11 wt%. To do this, we dissolved cellulose in imidazolium ionic liquid, 1-ethyl-3-methylimidazolium acetate (EMImAc), which enables dissolving large amounts of cellulose. The influence of cellulose concentration and drying method on the morphology and properties of final porous cellulose materials is presented and discussed. We demonstrate that by varying drying method we can obtain versatile cellulose materials with tuned porosity, pore sizes and morphology.

## Experimental

### Materials

Microcrystalline cellulose (Avicel<sup>®</sup>, pH-101, degree of polymerization 180 as given by the manufacturer),

purchased from Sigma Aldrich, was used after drying at 50 °C under vacuum for at least 2 h. 1-ethyl-3-methylimidazolium acetate ionic liquid (EMImAc) was from BASF, and dimethyl sulfoxide (DMSO) and absolute ethanol were from Fisher Chemical. Water was distilled.

## Methods

### *Preparation of wet cellulose precursor*

Solutions based on 3–11 wt% of cellulose were prepared in a mixture of DMSO/EMImAc (60/40 wt/wt). This solvent composition enables the dissolution of cellulose in this concentration range, as reported previously (Le et al. 2014). First, dried microcrystalline cellulose was mixed with DMSO and heated at 70 °C under magnetic stirring for 2 h; then EMImAc was added and the mixture was kept at 70 °C under magnetic stirring for another 2–24 h depending on cellulose concentration. High viscosity solutions were placed under vacuum to remove air bubbles in order to avoid artefacts such as formation of “holes” or large macropores.

The resulting cellulose solutions, transparent and optically homogeneous, were poured into cylindrical plastic vials that served as molds. Once the solutions cooled down, ethanol was poured on the surface of solution in order to coagulate the dissolved cellulose. When coagulation was completed and ionic liquid washed out, the samples were then washed several times in distilled water to get white cellulose “aquagels”. These were the precursors for different drying routes. This procedure ensured the same state of all samples before drying.

### *Freeze-drying*

The freeze-drying of aquagels was performed in the Cryotec Cosmos 80 freeze-dryer (cold trap temperature –80 °C, pressure 40 mTorr) for 48 h. The samples obtained after freeze drying are called “cryogels”.

Two kinds of cryogels were prepared: with unidirectional pre-freezing and not. The unidirectional pre-freezing was done in glass vials which bottoms were in contact with liquid nitrogen (–196 °C), whilst the sides of the vials were insulated with polystyrene foam to prevent heat transfer from the side walls. The pre-

frozen aquagels were then immediately put into the freeze-dryer and water was sublimated. Such samples are hereafter referred to as “cryogels (unidirectional freezing)”. Aquagels that did not undergo the pre-freezing procedure were simply put into the freeze-dryer and then freeze-dried. These samples are thus called “cryogels (freeze-dryer)”.

### *Vacuum drying*

The vacuum drying of aquagels was done in a standard vacuum oven at room temperature for 48 h. The resulting samples are called “xerogels”.<sup>1</sup>

### *Supercritical (sc) CO<sub>2</sub> drying*

Prior to drying, the aquagels were washed several times in ethanol to remove water. The supercritical CO<sub>2</sub> drying was carried out in Separex S.A.S. (France) at 110 bars and 45 °C. Such samples are called “aerogels”.<sup>2</sup>

### *Bulk density*

The bulk density was measured using the Micromeritics GeoPyc 1360 Envelope Density Analyzer with the DryFlo<sup>®</sup> powder as fluid medium. Each sample was measured in 5 cycles with applied force of 25 N. The standard deviation of the measured values is  $\pm 0.002$  g/cm<sup>3</sup>.

### *Specific surface area*

The specific surface area was determined by measuring N<sub>2</sub>-adsorption isotherm at 77 K with the ASAP 2020 (Micromeritics) and using the equation by

<sup>1</sup> Authors understand that the so-obtained xerogels, as it will be shown later, are not fitting the classical definition of xerogels which should retain 15–50 % porosity, possess small mesopores and micropores and have specific surface area of several hundreds of m<sup>2</sup>/g. However, for the sake of simplicity, the term “xerogel” is kept in this work.

<sup>2</sup> The term «aerogel» is also not well adapted for the case of polysaccharide-based ultralight materials obtained via drying with sc CO<sub>2</sub>. Classical aerogels are mesoporous/small macroporous materials while polysaccharide-based “aerogels” possess from large to very large macropores, up to few microns, which leads to specific surface area two to four time lower than that of classical (e.g. silica) aerogels. For the sake of simplicity we keep the term “aerogel” in this work.

Brunauer, Emmett and Teller (BET equation) (Brunauer et al. 1938). The samples were measured after being degassed for 5 h at 70 °C.

### Scanning electron microscopy (SEM)

Morphological analysis of the dry celluloses was performed in Zeiss Supra™ 40 FEG scanning electron microscope with secondary electrons detector. Prior observations all the samples were metallized with 7 nm of platinum. The acceleration voltage used was 3 kV.

Average pore sizes were studied using the image analysis software Archimed™ (Microvision Instruments). At least 100 sizes on each of three different SEM images per formulation were measured. The minimal resolution was 0.1 μm.

## Results and discussion

### Sample shrinkage, density and porosity

After coagulation in ethanol and several washing cycles in distilled water, white cellulose “aquagels” were obtained as shown in Fig. 1. Such wet aquagels were then dried by one of the techniques mentioned in Methods section; the resulting dry samples are also shown in Fig. 1. Aerogels and both kinds of cryogels are white and opaque, whereas xerogels are yellowish, translucent and much more shrunk.

To prepare aero- cryo- and xerogels we used cellulose solutions with concentrations ranging from 3 to 11 wt%: monoliths are not formed from solutions with lower cellulose content because the overlap concentration is around 1–1.5 wt% for microcrystalline cellulose (Gericke et al. 2009), and solutions of higher concentrations are rather difficult to handle due to their high viscosity. It is also worth noting that

direct freeze-drying led to breakage of the 3 wt% sample most probably because precursor of low cellulose concentration was unable to resist high and heterogeneous stresses developed during water sublimation. All the other samples were monolithic.

Coagulation and drying steps lead to certain volume shrinkage compared to the volume occupied by the initial solution in the mold. The volume shrinkage was calculated for all the monolithic samples as follows:

$$\text{Volume shrinkage}(\%) = 100 \times \left( 1 - \frac{V_x}{V_{sol}} \right) \quad (1)$$

where  $V_x$  is the sample volume at a given step (aquagel or after drying) and  $V_{sol}$  is the volume of cellulose solution before coagulation. All volume shrinkages after each step are shown in Fig. 2 as a function of cellulose concentration and drying method, and the final values are summarized in Table 1.

Coagulation of dissolved microcrystalline cellulose induces volume shrinkage of up to 20 vol% at 3 wt% cellulose concentration in solution. This value decreases to around 5 vol% for all the other higher cellulose concentrations. Additional volume shrinkage can be observed after drying of the coagulated cellulose: it is enormous for vacuum drying, followed by rather high shrinkage for sc CO<sub>2</sub> drying and low shrinkage for freeze-drying.

Evaporative vacuum drying is slow and induces strong capillary pressure applied on pore walls: it is proportional to liquid/solid contact angle and liquid/gas surface tension and inversely proportional to network pore size. In the case of cellulose “aquagel”, the first two components are high because cellulose is hydrophilic and water surface tension is high. In addition to capillary stresses, densification is due to strong hydrogen bonds that are formed between numerous hydroxyl groups which are present on cellulose chain. As a result, the overall volume shrinkage in cellulose xerogels is close to and above



**Fig. 1** Examples of an aquagel and samples after drying with different techniques (aerogel, cryogels and xerogel) obtained from 7 wt% cellulose solution

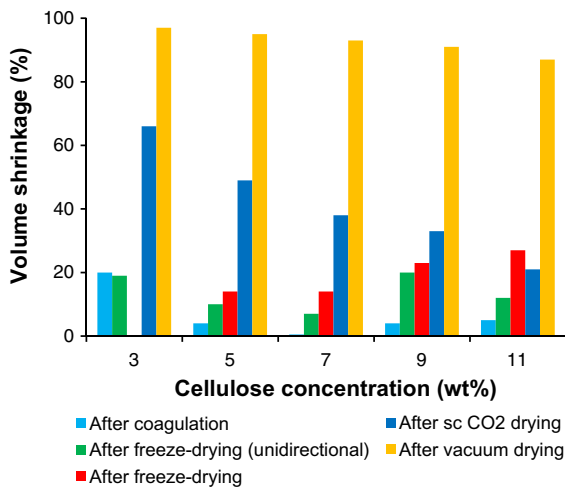


**Fig. 2** Volume shrinkage after each processing step of cellulose samples as a function of cellulose concentration for various drying methods; the *error* is around  $\pm 10$  vol% (not shown not to overload the graph)

90 vol%. The volume shrinkage of xerogels seems to slightly decrease with increasing cellulose concentration suggesting that the higher the quantity of

cellulose, the stronger the network and pore walls resist better the capillary stress.

Drying with supercritical CO<sub>2</sub> generates much lower volume shrinkage compared to vacuum drying except for aerogels prepared from solutions of low cellulose concentration. The shrinkage is concentration-dependent: it decreases with increasing cellulose concentration from 66 to 21 vol% as the cellulose concentration increases from 3 to 11 wt%. The decrease of shrinkage with the increase of cellulose concentration in aerogels was reported by Hoepfner et al. (2008). The values obtained in this work are rather high for a process which is supposed to have theoretical zero capillary pressure because liquid/gas surface tension is zero. One of the reasons could be a significant difference in the solubility parameters of cellulose (39 MPa<sup>0.5</sup>) and CO<sub>2</sub> (around 5 MPa<sup>0.5</sup>) (Barton 1991). Processing conditions, among which depressurization step plays the important role, also influence volume shrinkage. Similar values of the overall volume shrinkage from cellulose solution to cellulose aerogel, around 40–70 vol%, were reported

**Table 1** Total volume shrinkage, bulk density, porosity and BET specific surface area of cellulose aero-, cryo- and xerogels

Sample	Cellulose concentration in solution (wt%)	Volume shrinkage (%)	Bulk density (g/cm <sup>3</sup> )	Porosity (%)	BET specific surface area (m <sup>2</sup> /g)
Aerogel	3	66	0.126	92	239
	5	49	0.130	91	282
	7	38	0.159	89	286
	9	33	0.175	88	291
	11	21	0.215	86	312
Cryogel (unidirectional freezing)	3	19	0.050	97	10
	5	10	0.073	95	14
	7	7	0.099	93	17
	9	20	0.132	91	18
	11	12	0.163	89	49
Cryogel (freeze-dryer)	3	Sample broken	0.053	96	11
	5	14	0.068	95	13
	7	14	0.099	93	16
	9	23	0.132	91	24
	11	27	0.164	89	62
Xerogel	3	97	1.427	5	–
	5	95	1.470	2	–
	7	93	1.445	4	–
	9	91	1.468	2	–
	11	87	1.446	4	–

by Innerlohinger et al. (2006), Liebner et al. (2009) and Sescousse and Budtova (2009).

Freeze-drying, with and without pre-freezing, generates the lowest volume shrinkage among all the drying techniques discussed above. Contrary to other samples, volume shrinkage of both kinds of cryogels does not seem to evolve with cellulose concentration being around 10–20 vol%.

Bulk densities  $\rho_{bulk}$  of the cellulose aero-, cryo- and xerogels are summarized in Table 1 and are shown in Fig. 3 as a function of cellulose concentration. A theoretical density calculated for a hypothetical case of zero volume shrinkage is also shown for comparison. Porosity was calculated as follows:

$$Porosity(\%) = 1 - \frac{\rho_{bulk}}{\rho_{skeletal}} \quad (2)$$

where  $\rho_{skeletal} = 1.5 \text{ g/cm}^3$  being the skeletal density of cellulose.

The bulk density of all samples increases with increasing cellulose concentration, as expected. Xerogels, which undergo high volume shrinkage, have the highest bulk density as compared to those of the other samples. The bulk density of xerogels approaches the density of microcrystalline cellulose which is approx.  $1.5 \text{ g/cm}^3$  (Sun 2005). Therefore, the inner porosity of xerogels is very low, at the order of a few per cents (see

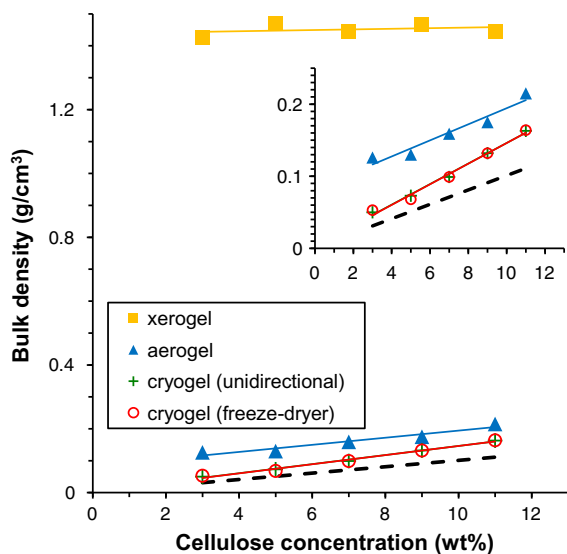


**Fig. 3** Bulk density of cellulose aero-, cryo and xerogels as a function of cellulose concentration; dashed line is theoretical density corresponding to hypothetical samples with zero volume shrinkage; *inset* zoom into low-density region

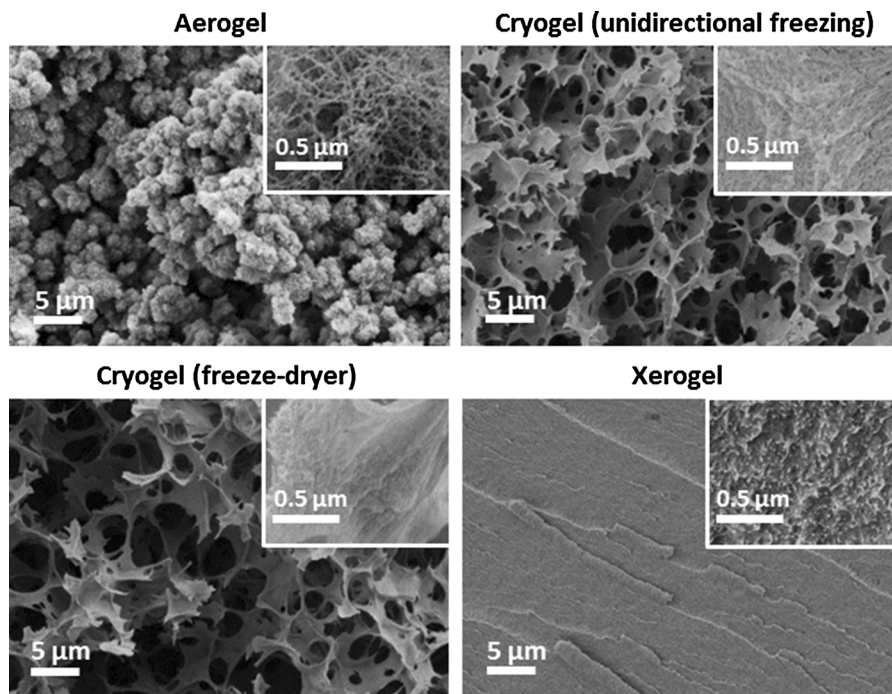
Table 1). The obtained dense xerogels are different from those reported by Ganesan et al. 2016 for emulsion-templated cellulose: the density of their xerogels was much lower,  $0.3\text{--}0.5 \text{ g/cm}^3$ , probably due to (1) the presence of large pores and channels which did not collapse during drying, and also (2) other fluids, ethanol and isopropanol, employed for evaporation. Aerogels, whose shrinkage is considerably lower than that of xerogels, have densities ranging from  $0.126$  to  $0.215 \text{ g/cm}^3$ . These values are comparable to the bulk densities of other cellulose II based aerogels already reported in the literature (Innerlohinger et al. 2006; Gavillon and Budtova 2008; Hoepfner et al. 2008; Sescousse et al. 2011b; Ganesan et al. 2016). Because the volume shrinkage is concentration-dependent (Fig. 2), the linear trend correlating cellulose concentration in solution and aerogel density does not go through the origin (see inset in Fig. 3). Finally, due to the very low volume shrinkage during freeze-drying, both kinds of cryogels have extremely low bulk densities that are almost equal to the theoretical one calculated for zero volume shrinkage. For example, with 3 wt% cellulose in solution, the bulk density as low as  $0.050 \text{ g/cm}^3$  was obtained for the cryogel (unidirectional freezing) corresponding to 97 % of porosity. Comparable values have already been reported for cellulose II based cryogels synthesized from cellulose of higher molecular weight dissolved in calcium thiocyanate (Hoepfner et al. 2008) and for porous cellulose made from microfibrillated cellulose (Schaqui et al. 2010).

#### Morphology and specific surface area

The morphology of cellulose aero-, cryo- and xerogels was studied by SEM. Figure 4 shows the inner textures observed on samples made from 5 wt% cellulose solution. These pictures are representative of morphologies observed for all the other cellulose concentrations.

It is clear that the inner texture of the cellulose materials strongly depends on the drying technique used. Aerogels, which were prepared by drying with  $\text{sc CO}_2$ , present cauliflower-like arrangement of cellulose: an agglomeration of small shaggy beads. The latter have fine nanostructured fibrillated texture as shown in the inset. Such morphology is typical for aerogels prepared from direct coagulation of dissolved cellulose (Sescousse et al. 2011b; Demilecamps et al.

**Fig. 4** SEM images of cellulose aero-, cryo- and xerogel made from 5 wt% cellulose solution



2015). Classical methods such as mercury porosimetry and nitrogen adsorption (BJH approach) do not allow obtaining pore size distribution in cellulose aerogels: in the first case, aerogels are compressed under mercury pressure and mercury is not entering pores, and in the second, BJH does not allow obtaining pore sizes in a wide range, from few tens of nanometers to few microns. As roughly estimated from SEM images, the average distance between the cellulosic fibrils in the beads is of the order of tens of nanometers and fibrils' thickness is around 20–30 nm. The average size of the beads is of few micrometers in diameter. Image analysis of aerogels prepared from solutions of different cellulose concentrations shows that bead's size decreases with increasing cellulose concentration from approximately 2.3 μm for aerogels from 3 wt% cellulose solution to 1.3 μm for 11 wt% solution.

Both kinds of cryogels have the same morphology which is typical for freeze-dried polysaccharide-based samples (Mattiasson et al. 2009) and very different from aerogels obtained via drying with sc CO<sub>2</sub> (Fig. 4). Freeze-drying leads to sheet-like cellulose network with large and interconnected pores of several micrometers in diameter due to ice growth during water freezing. The pore walls in cryogels are much thicker than in aerogels, around 80 nm, and they do

not seem to be mesoporous or with small macropores as can be seen from the images of higher magnification (Fig. 4), and also deduced from low specific surface area values (Table 1). All fine structure formed during cellulose coagulation and preserved when drying with sc CO<sub>2</sub> is completely lost during freeze-drying. The pressure generated during ice crystal growth and applied on pore walls compresses the fibrils together resulting in “flat” non-porous walls.

Supposing that the majority of pores in cryogels are “seen” with a high-resolution SEM, we measured their diameter. This approach is acceptable because cryogels have only very large macropores as it will be demonstrated further with BET analysis. For cryogels of each type and of each cellulose concentration pore sizes were analyzed at different distances from sample bottom in order to check the influence of temperature gradient in the unidirectionally frozen samples. An example of pore size distribution for cryogels made with unidirectional freezing and frozen directly in the freeze-dryer is shown in Fig. 5.

In cryogels prepared without pre-freezing no noticeable influence of pore location (either in the vertical or in horizontal direction) on its size was detected. It was already reported that ice crystals vertically grown from the bottom-cooled surface

induce pore size increase along the vertical axis and formation of aligned channels in cellulose freeze-dried directly from NaOH–water–urea solution (Flauder et al. 2014), or microfibrillated cellulose (Sehaqui et al. 2010; Lee and Deng 2011) or cellulose or chitin nanocrystals dispersed in a polymer solution (Köhnke et al. 2014; Zhou et al. 2014). However, because in our case cellulose is already coagulated before freeze-drying and thus the network structure is fixed, no aligned channels from the bottom to the top surface were observed. The latter is possible in solutions or suspensions. In the cryogels pre-frozen with a temperature gradient via ice-templating technique, the pore size was found to increase from the bottom-cooled surface to the warmer top surface (Fig. 5). For example, if taking as a representative pore size the arithmetic average value, in the case of 3 wt% cellulose-based cryogel (unidirectional freezing) the pore size increases from 4.3  $\mu\text{m}$  close to the bottom to 7.5  $\mu\text{m}$  close to the top surface. For 3 wt% cryogel directly frozen in the freeze-dryer the pore size remains constant (*approx.* 5.2  $\mu\text{m}$ ) within all the sample volume.

The influence of cellulose concentration on average pore diameter of cryogels is shown in Fig. 6. For both types of cryogels pore's size decreases with increasing

concentration. For example, for pore size in cellulose cryogel (freeze-dryer) decreases from almost 6  $\mu\text{m}$  to around 1.5  $\mu\text{m}$  when the concentration goes from 3 to 11 wt%; the same trend is observed for pre-frozen samples. Overall, using unidirectional pre-freezing and/or varying cellulose concentration allows tuning pore sizes in cellulose cryogels. A similar result, i.e. the decrease of pore size with the increase of cryogel density, was reported for microfibrillated cellulose (Sehaqui et al. 2010).

Finally, xerogels are, due to strong pores contraction during slow vacuum drying, very dense and their porosity is close to zero. No macro- or mesopores are visible on SEM images of xerogels (Fig. 4). As expected, vacuum drying cannot be used as drying technique for the preparation of porous non-modified cellulose materials.

To better understand the influence of cellulose concentration on aero- and cryogel morphology, specific surface area was measured using nitrogen adsorption and BET approach. The results are shown in Fig. 7 and the values are given in Table 1. The specific surface area of xerogels is very low for all cellulose concentrations explored in this study. It was found to be of the order of 1  $\text{m}^2/\text{g}$  which is at the limit of detection for this technique; the exact values are

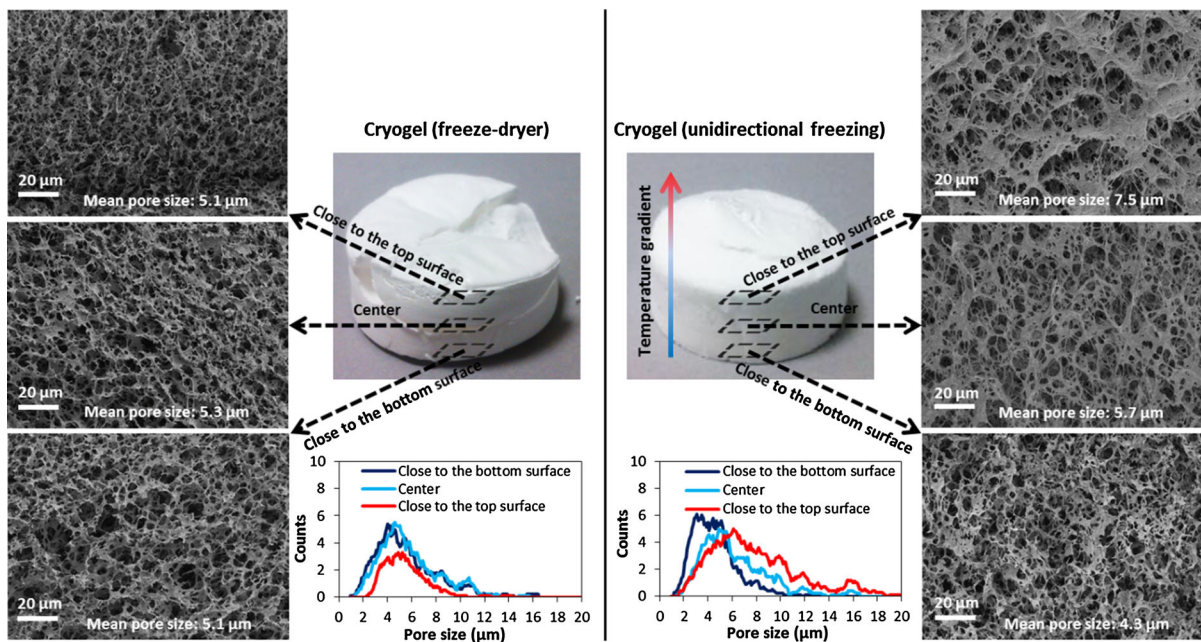
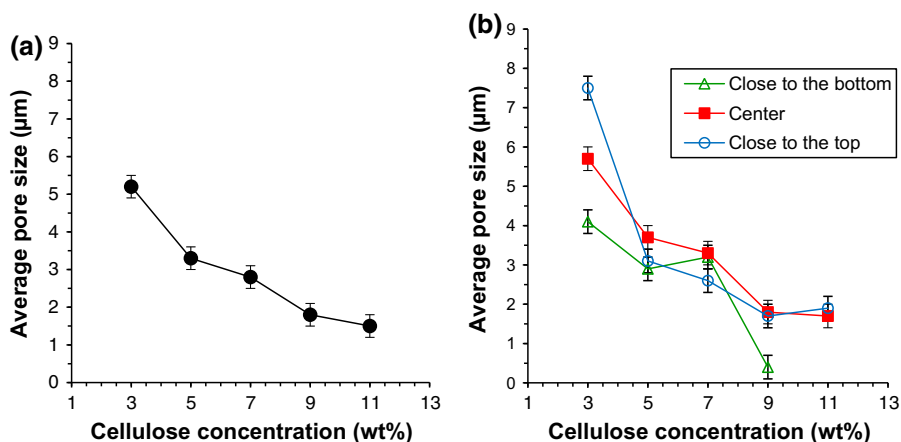


**Fig. 5** Morphology and pore size evolution along the vertical axis in cryogels prepared from 3 wt% cellulose solution



**Fig. 6** Pore size as a function of cellulose concentration in solution for (a) cryogels (freeze-dryer) and (b) cryogels (unidirectional freezing); lines are given to guide the eye



thus not given. This result is in good accordance with high volume shrinkage and high bulk density values as well as with SEM observations.

Cellulose aerogels have rather high specific surface area, in the range of 240–310 m<sup>2</sup>/g, similar to other cellulose II based aerogels (Hoepfner et al. 2008; Aaltonen and Jauhiainen 2009; Sescousse et al. 2011b; Trygg et al. 2013; Demilecamps et al. 2015; Ganesan et al. 2016), and it increases with the increase of cellulose concentration (Fig. 7). A similar trend was reported for aerogels prepared from cellulose dissolved in NaOH–urea–water, coagulated in acid and dried with sc CO<sub>2</sub> (Trygg et al. 2013). High specific

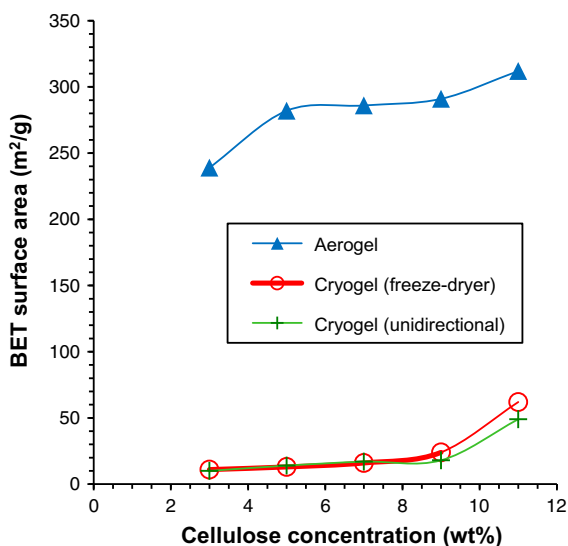


**Fig. 7** Specific surface area of cellulose aero- and cryogels as a function of cellulose concentration in solution; the lines are given to guide the eye

surface area of cellulose aerogels is due to their multi-scale nanostructure shown by SEM (Fig. 4).

Both types of cryogels with micrometer-size pores have specific surface areas one order of magnitude lower than that of aerogels, around few tens of m<sup>2</sup>/g, as typically observed for cellulose-based materials with very large macropores (Hoepfner et al. 2008; Pääkkö et al. 2008; Sehaqui et al. 2010; Ganesan et al. 2016). Moreover, cryogels specific surface area increases from approx. 10 to 50–60 m<sup>2</sup>/g with increasing cellulose concentration from 3 to 11 wt%, the same trend as observed for cellulose aerogels.

With the increase of cellulose concentration two major options in morphology evolution are possible: (1) increase of pore walls thickness and (2) decrease of pore size without pore wall thickness evolution. A schematic presentation is shown in Fig. 8. The experimental results show that the increase of cellulose concentration in aero- and cryogels leads to a decrease of pore size in cryogels and a decrease of bead size in aerogels as observed with SEM, and an increase of specific surface area recorded with BET analysis in both cases. We can thus conclude that the increase of cellulose concentration leads to a “division” of pores into smaller ones, both in aerogels and cryogels, keeping pore wall thickness roughly unchanged. Each method confirms the result obtained with the other.

## Conclusions

Ultralight and porous monolithic cellulose materials were prepared and characterized. The synthesis consisted of cellulose dissolution in ionic liquid/DMSO

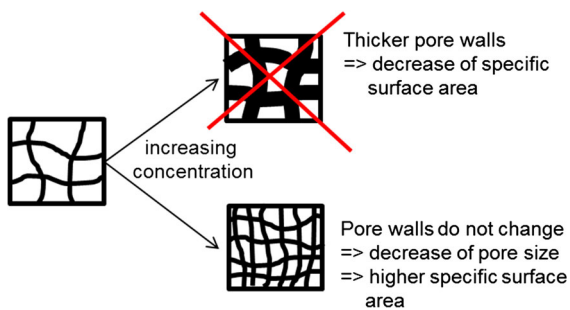


**Fig. 8** Schematic presentation of possible morphology evolution in a porous matter with the increase of polymer concentration

mixture followed by coagulation in ethanol and drying. Cellulose concentrations in the range of 3 to 11 wt% were explored. Starting from the same coagulated precursor, three different drying methods were employed: supercritical CO<sub>2</sub> (aerogels), freeze-drying (cryogels) and vacuum drying (xerogels).

Vacuum drying induced strong pore collapse resulting in samples with very low porosity, not-measurable specific surface area and densities close to that of microcrystalline cellulose. Supercritical CO<sub>2</sub> drying yield nanostructured aerogels with bulk densities between 0.12 and 0.215 g/cm<sup>3</sup> and specific surface area up to 300 m<sup>2</sup>/g. Freeze-drying gives highly macroporous cryogels with much lower specific surface areas (at the order of tens of m<sup>2</sup>/g) but which can be as light as 0.05 g/cm<sup>3</sup>. The difference in the density of aerogels vs. cryogels is due to sample volume contraction during drying step which is more pronounced for aerogels of low cellulose concentrations.

Cellulose aero- and cryogels bulk density and specific surface area were found to increase with increasing cellulose concentration. Such a behavior was explained by the decrease of pore size upon concentration increase while keeping the pore wall thickness unchanged. This result is confirmed by SEM observations which showed the decrease of pore size with the increase of cellulose concentration.

There is a great difference between aerogels and cryogels morphology. Aerogels are hierarchically structured with pore size varying from few tens of nanometers between the fibrils to few microns between the “hairy” beads. Cryogel morphology is a sheet-like cellulose network with large interconnected pores of several microns. The only reason of this

difference is the drying method: drying with sc CO<sub>2</sub> preserves the inner porosity formed during coagulation despite overall sample contraction while the growth of ice crystals during freezing leads to compact pore walls and large pores.

Contrary to the morphology reported for cryogels made from polysaccharide solutions or from nanocellulose dispersed in aqueous medium, no large and long channels are formed in cellulose II cryogels. The reason is the coagulation step which is “fixing” the overall structure. Finally, it is also possible to vary the pore size within one cryogel sample by applying a unidirectional freezing before freeze-drying. This allows decreasing pore size in the direction of temperature gradient, from lower to higher temperatures.

In summary, we demonstrated that it is possible to tune the properties of porous cellulose materials by varying cellulose concentration and the drying method. Depending on the properties and morphology, such materials may have a wide range of applications. For example, thanks to their biocompatibility, cellulose aerogels and cryogels could be used in biomedical field as matrices for controlled drug release or in tissue engineering. It is also possible to imagine hybrid or composite materials (cellulose-organic or cellulose-inorganic) in which the pores of cellulose are filled with another substance resulting in an interpenetrated network. The overall properties will then depend on the synergy and interactions of the components and lead to novel applications (adsorption and/or separation of gases, matrices for catalysis, etc.).

**Acknowledgments** This work was performed in the frame of European project “AEROWOOD”, WoodWisdom Net+ EC program, and supported by French ministry of agriculture, food processing and fishing.

## References

- Aaltonen O, Jauhiainen O (2009) The preparation of lignocellulosic aerogels from ionic liquid solutions. *Carbohydr Polym* 75:125–129
- Barton AFM (1991) Handbook of solubility parameters and other cohesion parameters, 2nd edn. CRC Press, Boca Raton
- Brunauer S, Emmett PH, Teller E (1938) Adsorption of gases in multimolecular layers. *J Am Chem Soc* 60:309–319
- Demilecamps A, Beauger C, Hildenbrand C, Rigacci A, Budtova T (2015) Cellulose–silica aerogels. *Carbohydr Polym* 122:293–300

- Flauder S, Heinze T, Müller F (2014) Cellulose scaffolds with an aligned and open porosity fabricated via ice-templating. *Cellulose* 21:97–103
- Ganesan K, Dennstedt A, Barowski A, Ratke L (2016) Design of aerogels, cryogels and xerogels of cellulose with hierarchical porous structures. *Mater Design* 92:345–355
- García-González CA, Alnaief M, Smirnova I (2011) Polysaccharide-based aerogels—promising biodegradable carriers for drug delivery systems. *Carbohydr Polym* 86:1425–1438
- Gavillon R, Budtova T (2008) Aerocellulose: new highly porous cellulose prepared from cellulose–NaOH aqueous solutions. *Biomacromolecules* 9:269–277
- Gericke M, Schlufner K, Liebert T, Heinze T, Budtova T (2009) Rheological properties of cellulose/ionic liquid solutions: from dilute to concentrated states. *Biomacromolecules* 10:1188–1194
- Guilminot E, Gavillon R, Chatenet M, Berthon-Fabry S, Rigacci A, Budtova T (2008) New nanostructured carbons based on porous cellulose: elaboration, pyrolysis and use as platinum nanoparticles substrate for oxygen reduction electrocatalysis. *J Power Sources* 185:717–726
- Hoepfner S, Ratke L, Milow B (2008) Synthesis and characterisation of nanofibrillar cellulose aerogels. *Cellulose* 15:121–129
- Innerlohinger J, Weber HK, Kraft G (2006) Aerocellulose: aerogels and aerogel-like materials made from cellulose. *Macromol Symp* 244:126–135
- Isikgor FH, Becer CR (2015) Lignocellulosic biomass: a sustainable platform for the production of bio-based chemicals and polymers. *Polym Chem* 6:4497–4559
- Klemm D, Heublein B, Fink HP, Bohn A (2005) Cellulose: fascinating biopolymer and sustainable raw material. *Angew Chem Int Ed* 44:3358–3393
- Kobayashi Y, Saito T, Isogai A (2014) Aerogels with 3D ordered nanofiber skeletons of liquid-crystalline nanocellulose derivatives as tough and transparent insulators. *Angew Chem Int Ed* 53:10394–10397
- Köhnke T, Elder T, Theliander H, Ragauskas AJ (2014) Ice templated and cross-linked xylan/nanocrystalline cellulose hydrogels. *Carbohydr Polym* 100:24–30
- Le KA, Rudaz C, Budtova T (2014) Phase diagram, solubility limit and hydrodynamic properties of cellulose in binary solvents with ionic liquid. *Carbohydr Polym* 105:237–243
- Lee J, Deng Y (2011) The morphology and mechanical properties of layer structured cellulose microfibril foams from ice-templating methods. *Soft Matter* 7:6034–6040
- Liebner F, Haimer E, Potthast A, Loidl D, Tschegg S, Neouze MA, Wendland M, Rosenau T (2009) Cellulosic aerogels as ultra-lightweight materials. Part 2: synthesis and properties. *Holzforschung* 63:3–11
- Liebner F, Haimer E, Wendland M, Neouze MA, Schlufner K, Miethe P, Heinze T, Potthast A, Rosenau T (2010) Aerogels from unaltered bacterial cellulose: application of scCO<sub>2</sub> drying for the preparation of shaped, ultra-lightweight cellulosic aerogels. *Macromol Biosci* 10:349–352
- Mattiasson B, Kumar A, Galeev IY (2009) Macroporous polymers: production, properties and biotechnological/ biomedical applications. CRC Press, Boca Raton
- Pääkkö M, Vapaavuori J, Silvennoinen R, Kosonen H, Ankerfors M, Lindström T, Berglund LA, Ikkala O (2008) Long and entangled native cellulose I nanofibers allow flexible aerogels and hierarchically porous templates for functionalities. *Soft Matter* 4:2492–2499
- Sehaqui H, Salajková M, Zhou Q, Berglund LA (2010) Mechanical performance tailoring of tough ultra-high porosity foams prepared from cellulose I nanofiber suspensions. *Soft Matter* 6:1824–1832
- Sehaqui H, Zhou Q, Ikkala O, Berglund LA (2011) Strong and tough cellulose nanopaper with high specific surface area and porosity. *Biomacromolecules* 12:3638–3644
- Sescousse R, Budtova T (2009) Influence of processing parameters on regeneration kinetics and morphology of porous cellulose from cellulose–NaOH–water solutions. *Cellulose* 16:417–426
- Sescousse R, Gavillon R, Budtova T (2011a) Wet and dry highly porous cellulose beads from cellulose–NaOH–water solutions: influence of the preparation conditions on beads shape and encapsulation of inorganic particles. *J Mater Sci* 46:759–765
- Sescousse R, Gavillon R, Budtova T (2011b) Aerocellulose from cellulose–ionic liquid solutions: preparation, properties and comparison with cellulose–NaOH and cellulose–NMMO routes. *Carbohydr Polym* 83:1766–1774
- Sun C (2005) True density of microcrystalline cellulose. *J Pharm Sci* 94:2132–2134
- Trygg J, Fardim P, Gericke M, Mäkilä E, Salonen J (2013) Physicochemical design of the morphology and ultrastructure of cellulose beads. *Carbohydr Polym* 93:291–299
- Zhang Z, Sèbe G, Rentsch D, Zimmermann T, Tingaut P (2014) Ultralightweight and flexible silylated nanocellulose sponges for the selective removal of oil from water. *Chem Mater* 26:2659–2668
- Zhou Y, Fu S, Pu Y, Pan S, Ragauskas AJ (2014) Preparation of aligned porous chitin nanowhisker foams by directional freeze-casting technique. *Carbohydr Polym* 112:277–283